A wide angle multiple beam lens for convex conformal arrays

Rasime UYGUROĞLU[1,*], **Abdullah Y. ÖZTOPRAK**[1,2]

[1] Department of Electrical and Electronic Engineering, Engineering Faculty, Eastern Mediterranean University,
Magusa, Mersin 10 Turkey

[2] Final International University, Girne, Mersin 10, Turkey

Abstract: Multifocal lenses have been widely used as multiple beam forming networks for linear and planar arrays, but are not suitable for large convex conformal arrays as they are not physically realizable for wide angle beams. In this study, a new lens design especially suitable for convex conformal arrays is introduced. The new lens has no perfect focal points, but there are a certain number of correct phases in each of the beam directions. The directional patterns of the radiating elements are also taken into account to improve radiation patterns for desired directions. It has been shown that the new lens can be designed for circular arc arrays with satisfactory radiation performance for parameters where the design of realizable multifocal lenses is not possible.

Key words: Convex curved array, multiple beam, multifocal lens, perfect focal point

1. Introduction

Lens fed array antennas have been used to obtain wideband, wide angle multiple beams for many radar and satellite communication systems [1-4], collision avoidance systems [5], and biomedical imaging systems [6]. Constrained lenses with multiple focal points have been introduced by Ruze [7] and Rotman and Turner [8]. The use of two-dimensional multifocal lenses, commonly known as Rotman lenses, is well established and they have been shown to be very effective for linear or planar arrays [9-11]. There have been many studies to improve the performance of these lenses [12-17]. Research has also been carried out on three-dimensional multifocal lenses [18,19]. Conformal array antennas are used on the surface of structures of different shapes in radar and communication applications [20]. We could trace only a small number of articles studying multiple beams for these arrays [21-23].

When multifocal lenses are used with convex conformal arrays, the achievable maximum angular scan is smaller compared with that of similar size linear arrays. In fact, as demonstrated in section 2 of this paper, it becomes impossible to design realizable wide angle multifocal lenses for large size convex curved arrays. A two-dimensional lens is introduced in this paper for conformal arrays that has no perfect focal points. The new lens is specifically suitable for convex curved radiating arrays. The method makes use of the fact that the antenna elements of the radiating array have directional patterns and some antenna elements have minimal radiation in certain beam directions. Instead of having perfect focal points, the new design has a number of radiating array points that have no phase errors in each beam direction. With the lens introduced in the present paper, it is possible to obtain much wider angular coverage for convex curved arrays compared with arrays fed by

---

*Correspondence: rasime.uyguroglu@emu.edu.tr

multifocal lenses. It must be mentioned here that there are other multiple beam lenses, namely R-2R and R-KR lenses, that have been used successfully with curved arrays. However, both R-2R [23] and RK-R [3,24] are very specific lens design methods, which means they can only be used with circular arrays and do not have flexible design parameters as all three design curves have to be circular arcs. The principles of the lens introduced in the present paper can be used to design multiple beam lenses for circular arc radiating arrays as well as other convex radiating arrays.

After the limitations of multifocal lenses for convex curved arrays are shown in section 2, the new lens is introduced and analyzed in section 3. Radiation patterns are also presented in section 3 to show the wide angular coverage of the new lens. All designs in the present paper are obtained by using ray optics principles and path length equality from the feed point to the phase front.

2. Multifocal lenses

2.1. Design principles

A multifocal lens can be considered to consist of three antenna arrays on three curves: feed array, inner curve array, and outer curve array, as demonstrated in Figure 1. The array elements on the feed array that determine the beam directions are referred to as 'feed elements' and the array elements on the inner and outer curves of the lens are referred to as 'antenna elements' herein. The array on the outer curve is the radiating array. The antenna elements on the inner curve are connected to the antenna elements on the outer curve by varying lengths of transmission lines. A certain number of points on the feed array curve are designed to be focal points such that these feed points produce perfect phase fronts in particular directions. The beams produced by feed elements in between the focal points do not have ideal phase fronts but have some phase errors. If significant, these phase errors may cause beam deterioration (lower gain, higher sidelobes etc.). We shall discuss two-dimensional designs in this paper. For two-dimensional lenses, there are four possible variables for each dimension on the outer curve: the dimensions of the outer lens curve and dimensions of the inner curve, and the length of the transmission line between the associated points on the two curves of the lens. Thus if we consider a two-dimensional lens with no constraints on the shape of the inner curve or the outer curve of the lens, or the lengths of the transmission lines, the maximum number of focal points is four. If it is required that the outer curve has a certain shape, such as linear or circular, then the number of focal points drops to three [8].

The geometry of a two-dimensional multifocal lens with three focal points having a constrained nonlinear outer curve is given by Figure 1.

The design equations for this multifocal lens are given below:

$$\overline{F_1P} + \omega + \zeta_1 = f_1 + \omega_0 \tag{1}$$

$$\overline{F_0P} + \omega - x' = f_0 + \omega_0 \tag{2}$$

$$\overline{F_2P} + \omega + \zeta_2 = f_1 + \omega_0 \tag{3}$$

$$\zeta_1 = y' \sin\theta_0 - x' \cos\theta_0 \tag{4}$$

$$\zeta_2 = -(y' \sin\theta_0 + x' \cos\theta_0) \tag{5}$$

F_0, F_1, and F_2 are the three focal points and f_0 is the focal length for the central focal point F_0. f_1 is the focal length for the outer focal points F_1 and F_2. For a feed point placed at F_0 all path lengths to the
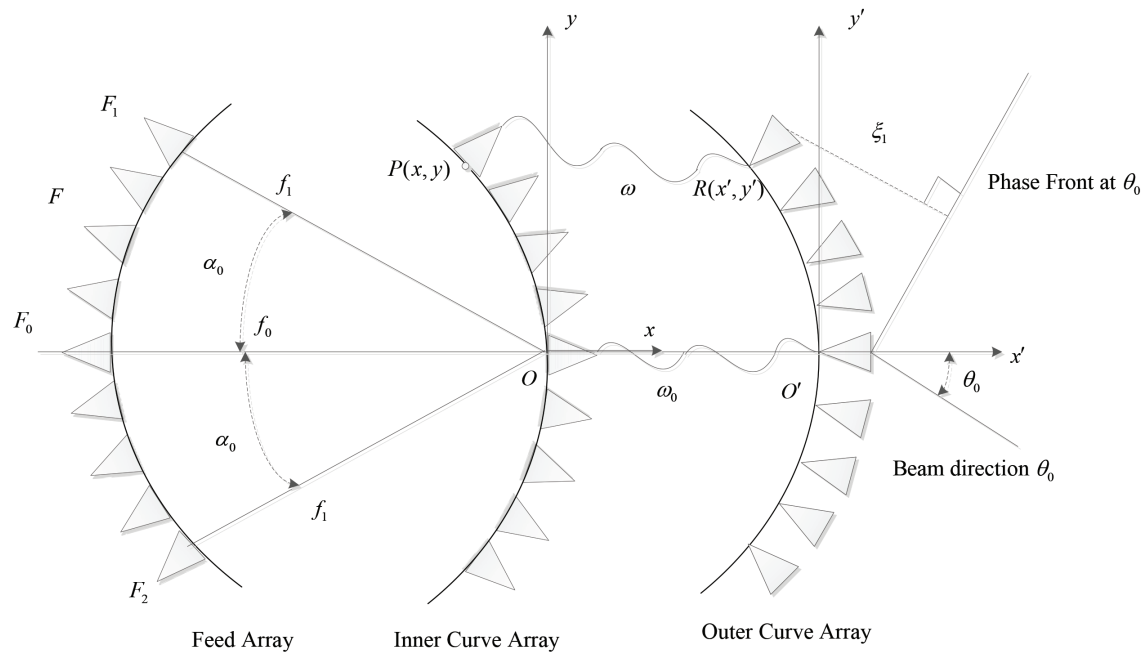
Figure 1. Mathematical model of the multifocal lens.

phase front at the broadside ($\theta = 0^o$) are equal, while for feed points at F_1 and F_2 path length equality is for phase fronts offset by θ_0 angle from the broadside. The points F_1 and F_2 are at an angular position α_0 from F_0 as shown in Figure 1. $P(x, y)$ is a general point on the inner curve and $P(x', y')$ is a general point on the outer curve. P and R are connected by a transmission line of length ω. ω_0 is the length of the transmission line at the center of the lens. For each point on the inner curve Equations (1), (2), and (3) can be solved for x, y, and ω to obtain the inner curve and the associated transmission line lengths.

2.2. Multifocal lens inner curves

Numerical solutions of the above three equations have been obtained to analyze the multifocal lens. All lengths are normalized to the central focal length f_0. Figure 2 shows the feed array curve and the three inner curves are for one linear and two circular outer curves with radii of $r = 0.750$ and $r = 0.414$ subtending total angles of 100° and 180°, respectively. For all three cases $f_1 = 1$, $f_0 = 1$, $\theta_0 = 60^o$, $\alpha_0 = 45^o$ and the arc length of the outer curve is 1.3. These examples show that the inner curve bends inwards as the convex outer curve becomes more and more curved, which corresponds to smaller. It can be observed that the design for the linear radiating array is realizable, as the inner curve elements are not blocking each other for outermost feed elements. On the other hand, although it is possible to obtain mathematical solutions for the two curved radiating arrays ($r = 0.750$ and $r = 0.414$) the designs are not physically realizable as the inner curve is bent inwards such that some of the antenna elements placed on the inner curve would be blocking other antenna elements on the same curve for the outermost feed elements (for example, for feed element F the element A on the inner curve would be blocking the element B on the inner curve as shown in Figure 2). This fact limits the angular coverage of multifocal lenses for convex curved radiating arrays.
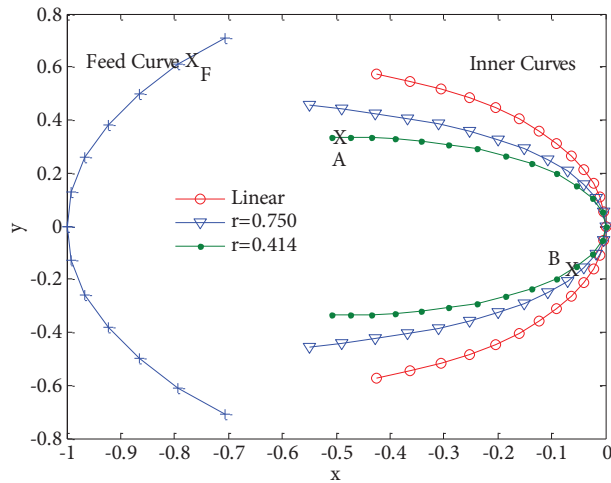
Figure 2. Inner curves for the multifocal lens.

3. Wide angle lens for curved array

3.1. Design principles

The new lens introduced in this section has no perfect focal points, and so there are no points on the feed array that produce perfect phase fronts. On the other hand, for each beam direction there is a certain number of radiating array elements that have no phase errors.

For a two-dimensional lens, it is possible to obtain a lens design such that each point on the inner curve has no phase errors for four chosen beam directions. Consequently for each beam direction, there are four points on the inner curve that has no phase errors, in addition to the center point of the lens. The number of no phase error points decreases to three if the outer curve of the lens is constrained to have a certain shape (linear, circular, etc.). This three equal phase point, two-dimensional design is the counterpart of the Rotman Lens, and, as will be shown later, wider angle designs are possible with this new lens for convex outer curves.

The directional pattern of the radiating array antenna elements is another factor taken into account for the design of this lens. The lens design parameters are chosen such that for a particular beam the antenna elements having large phase errors have minimum or no radiation in the beam direction, due to the directional pattern of the elements. In this way, the beam deterioration is kept to a minimum for all directions. Feed elements of the lens can be pointed towards low phase error antenna elements of the inner curve array. This further reduces the power transferred to the antenna elements of higher phase error, so that the amplitude of the corresponding radiating array antenna elements is low.

The geometry of the lens is shown by Figure 3. The (x, y) coordinate system is used for the feed array curve and the inner curve. The (x', y') coordinate system is used for the radiating array and the beam directions. The two coordinate systems are independent of each other. R is a general point on the outer curve and it is connected to a point P on the inner curve by a transmission line of length ω. ω_0 is the length of the transmission line between the center elements of the inner curve array and the outer curve array. The feed array is a circular array with a radius of f_0. A general point F_0 on the feed array curve at an angular position α_0 has an associated beam angle θ_0 and an associated outer curve array point at angular position of γ, where $\theta_0/\gamma = C_1$ and $\theta_0/\alpha_0 = C_2$. The points P and R are connected by a transmission line of length ω. C_1 and C_2 are constants; they are used as design parameters. $\Delta\theta$ determines the beam angles of the other two beams

(θ_1 and θ_2), which relate to feed element positions F_1 and F_2 on the feed array curve:

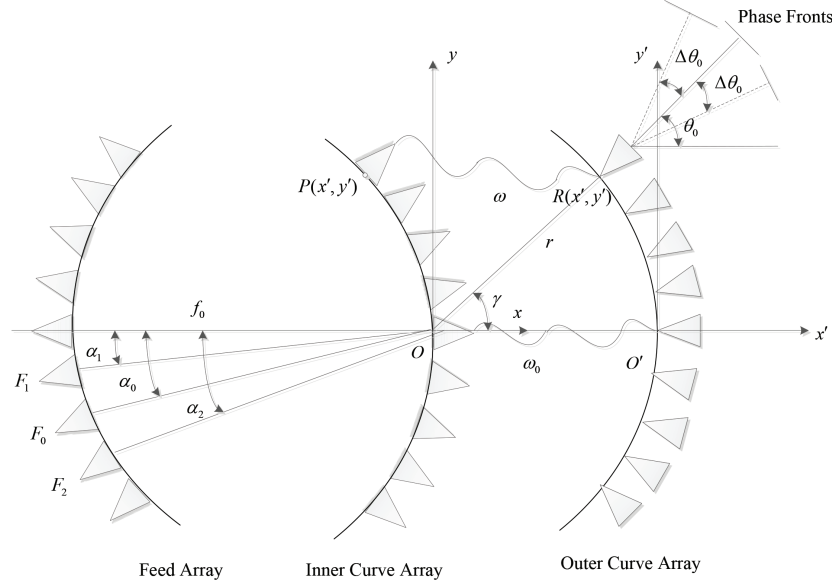$$\theta_1 = \theta_0 + \Delta\theta_0 \quad and \quad \theta_2 = \theta_0 - \Delta\theta_0 \tag{6}$$

Figure 3. Mathematical model of the new lens.

The angular positions of F_1 and F_2 (α_1 and α_2) are related to beam angles θ_1 and θ_2 as follows:

$$\alpha_1 = \theta_1/C_1 \tag{7}$$

$$\alpha_2 = \theta_2/C_1 \tag{8}$$

The phase from F_1, F_0, and F_2 to the phase front at θ_1, θ_0, and θ_2 are going to be equal to the constant (f_0, ω_0), which is the path length for the center element from the feed array to the phase front. The path length equalities are then

$$\overline{F_1P} + \omega + \zeta_1 = f_0 + \omega_0 \tag{9}$$

$$\overline{F_0P} + \omega + \zeta_0 = f_0 + \omega_0 \tag{10}$$

$$\overline{F_2P} + \omega + \zeta_2 = f_0 + \omega_0, \tag{11}$$

where

$$\zeta_1 = -(y'\sin\theta_1 + x'\cos\theta_1) \tag{12}$$

$$\zeta_0 = -(y'\sin\theta_0 + x'\cos\theta_0) \tag{13}$$

$$\zeta_2 = -(y'\sin\theta_2 + x'\cos\theta_2) \tag{14}$$

After substituting ζ_1, ζ_0, and ζ_2 into Equations (9), (10), and (11) solutions can be obtained for x, y, and ω. Thus, for each outer curve point defined by γ, we can obtain x, y, and ω values, which gives us the inner curve and the associated transmission line lengths. We must note here that for each beam direction there are four points on the outer curve (including the center point), which has no phase errors at the phase front. The design parameters of the lens (C_1, θ_0, $\Delta\theta$) should be chosen such that the radiating antenna elements have significant radiation in the directions in which they have no or low phase errors.

3.2. Lens analysis

Figure 4 shows two inner curves for the multifocal lens and the new lens, having the same design parameters. The design parameters are $\alpha_0 = 45^o$, $\theta_0 = 50^o$, $f_1 = f_0 = 1$, and $r = 0.75$. The length of the outer curve is $1.3f_0$ and the total angle subtended by the outer curve is 100°. $\Delta\theta = 40^o$ for the new lens. It is clear from Figure 4 that for this example it is feasible to obtain a physically realizable inner curve for the new lens, while it is not so for the multifocal lens. Although these results are for a particular design, they are typical for convex large arrays.
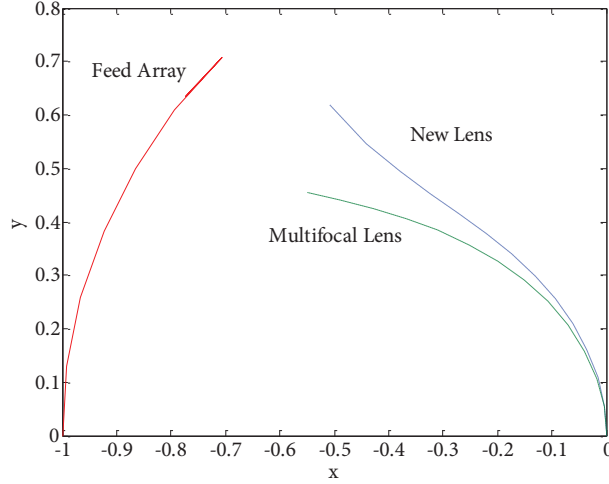

Figure 4. Comparison of the inner curves for the multifocal lens and the new lens.

Path length error Δl can be defined as the difference in the path from a general point F at an angular position α on the feed array curve to the phase front at θ, through a general point P and from the same point F through the center point O of the inner curve to the phase front at θ. Therefore, the path length error equation is

$$\Delta l = \overline{FP} + \omega + \zeta - \overline{FO} - \omega_0 \tag{15}$$

Path length errors determine the phase errors at the phase fronts. Large phase errors cause deterioration in the radiation patterns. Figure 5 shows the comparison of path length errors of the $\theta = 25^o$ beam for the two lenses given above. At 25° the multifocal lens has no blockage of inner curve elements. The path length errors for the new lens are small for those antenna elements that would have significant contribution in the direction of the beam, while the path length errors are very large for the noncontributing or the low contributing elements. The reverse is observed for the multifocal lens; where it matters most the path length errors are large. Figure 6 shows the path length errors for the above wide angle lens at three different beam directions 0°, 25°, 50°. It can be observed that as the beam moves to the right of the array the path length errors for the elements (with large phase errors) on the left of the array increase. Due to radiating antenna element patterns, these elements have a very small contribution in the main beam direction and so they do not cause significant beam deterioration.

3.3. Radiation patterns

Sample calculated radiation patterns have been obtained to show that the new lens can produce wide angle beams. These radiation patterns cannot be compared with the multifocal lens radiation patterns of the same
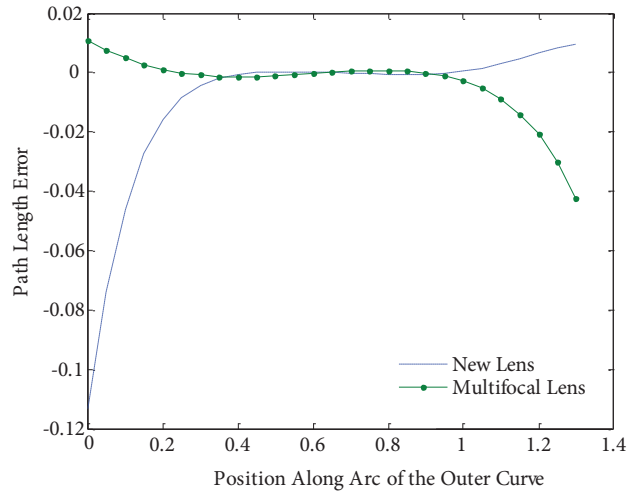
Figure 5. Comparison of the path length errors for the multifocal lens and the new lens.
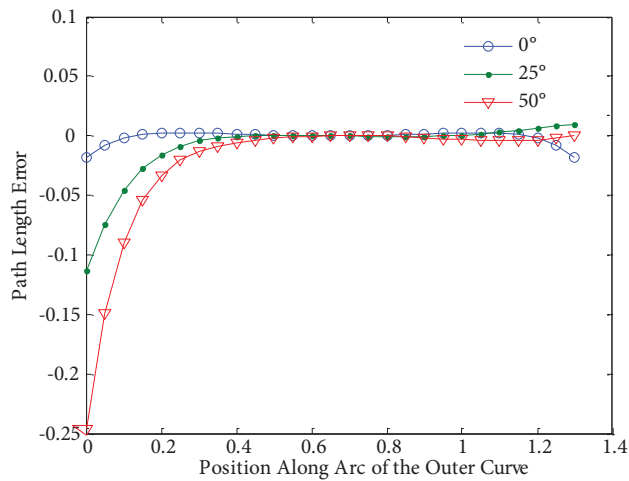

Figure 6. Path length errors for different beam positions of the new lens.

parameters as it is not possible to design realizable multifocal lenses for beams at large angles (see Figure 4). The radiation patterns for a two-dimensional 27 element array of $f = 7.5\lambda$ are given in Figure 7. The design parameters of this lens are the same as those of the lens analyzed in section 2. The feed elements of the feed array and the antenna elements of the inner and outer curve arrays are chosen to be $\lambda/2$ wide apertures having radiating patterns of [25]

$$E = E_0 \cos\theta' \left(\frac{\sin(\frac{\pi}{2}\sin\theta')}{\frac{\pi}{2}\sin\theta'}\right), \tag{16}$$

where E is the electric field intensity, E_0 is the magnitude of E, and the angle θ' is measured from the perpendicular to the axis of the antenna elements. No mutual coupling is taken into account. It can be observed that very reasonable beams are obtained for up to the maximum design angle of 50°, but there is a drop in the peak level of the outer beams. This drop is mainly due to the fact that a smaller number of radiating array elements contribute for these beams and as the effective aperture size of the radiating array is smaller in these directions.
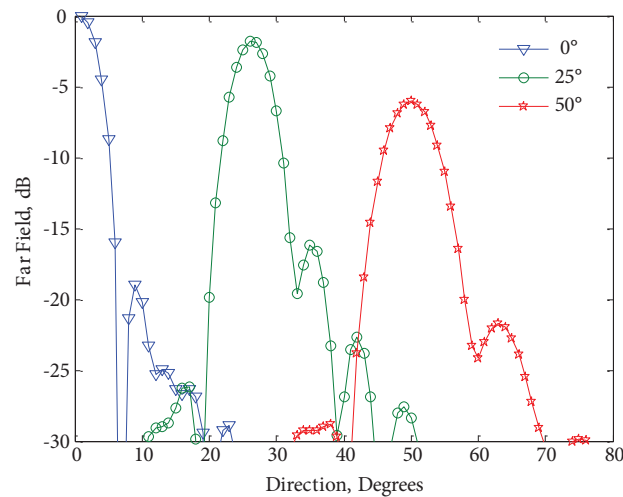
Figure 7. Radiation patterns for the new lens for $\theta_m ax = 50^o$.

These results indicate that, unlike multifocal conventional lenses, the new lens introduced in this paper can be used for convex nonlinear arrays at wide angles.

4. Conclusion

The paper introduces a new method for designing multiple beam lenses that are suitable for conformal convex radiating arrays. Lens design equations, lens curves, and path length errors have been presented for conventional multifocal bootlace lenses, as well as for the new lens.

It is shown that the conventional multifocal lenses are not suitable for large curved convex radiating arrays when wide angle beams are required.

The results of the study of the new lens show that it is possible to obtain physically realizable lenses as well as having beams that do not show significant deterioration.

References

[1] Archer D. Lens fed multiple beam arrays. *Microwave Journal*, 1975; 18: 18-37.

[2] Hall PS, Vetterlein SJ. Review of the frequency beamforming techniques for scanned and multiple beam antennas. *IEE Proceedings-H Microwaves, Antennas and Propagation*, 1990; 137 (18): 293-303. doi: 10.1049/ip-h-2.1990.0055

[3] Johnson RC, Jasik H. Antenna Engineering Handbook. *New York, NY, USA: McGraw-Hill Inc.*, 1993.

[4] Yan L, Shaoqiu X, Jiajia G. A review of wideband wide-angle scanning 2-D phased array and its applications in satellite communication. *Journal of Communications and Information Networks* 2018; 3 (1): 22-30. doi: 10.1007/s41650-018-0001-x 1990

[5] Metz C, Grubert J, Heyen J, Jacob AF, Janot S et al. Fully integrated automotive 2 radar sensor with versatile resolution. *IEEE Transaction on Microwave Theory and Technology* 2001; 49 (12): 2560-2566. doi: 10.1109/22.971650

[6] Jastram N, Filipovic DS. Wideband multibeam millimeter wave arrays. Memphis, *TN, USA, IEEE Antennas and Propagation Society International Symposium (APSURSI)*, 2014, pp. 741-742. doi: 10.1109/APS.2014.6904700

[7] Ruze J. Wide-angle metal plate optics. *Proceedings of the IRE* 1950; 38 (1): 53-59.

[8] Rotman W, Turner RF. Wide angle microwave lens for line source applications. *IEEE Transactions on Antennas and Propagation* 1963; 11 (6): 623-632. doi: 10.1109/TAP.1963.1138114

[9] Musa L, Smith, MS. Microstrip port design and sidewall absorption for printed Rotman lenses. *IEE Proceedings Microwaves Antennas Propagation* 1989; 136 (1): 53-58. doi: 10.1049/ip-h-2.1989.0009

[10] Hansen RC. Design trades for Rotman lenses. *IEEE Transactions on Antennas Propagation* 1991; 39 (4): 464-472. doi: 10.1109/8.81458

[11] Archer DH, Maybell MJ. Rotman lens development history at Raytheon electronic warfare systems 1967-1995. *in IEEE Antennas and Propagation Society International Symposium 2005; Washington DC, USA*, 2005; 2: 31-34. doi: 10.1109/APS.2005.1551927

[12] Schulwitz L, Mortazawi A. A new low loss Rotman Lens design using a graded dielectric substrate. *IEEE Transactions on Microwave Theory Techniques* 2008; 2 (12): 2734-2741. doi: 10.1109/TMTT.2008.2006802

[13] Shelton JP. Focusing characteristics of symmetrically configured bootlace lenses. *IEEE Transactions Antennas Propagation* 1978; 26 (4): 513-518. doi: 10.1109/TAP.1978.1141883

[14] Katagi T, Mano S, Sat S. An improved design method of Rotman lens antennas. *IEEE Transactions on Antennas and Propagation* 1984; 32 (5): 524-527. doi: 10.1109/TAP.1984.1143353

[15] Dong J, Zaghloul AL, Rotman R. Phase-error performance of multi-focal and non-focal two-dimensional Rotman lens designs. *IET Microwave Antennas and Propagation* 2010; 4 (12): 2097-2103. doi: 10.1049/iet-map.2009.0565

[16] Uyguroglu R, Ergün C, Oztoprak AY. Improved phase performance for Rotman lens. *International Journal of RF Microwave Computer- Aided Engineering* 2013; 23 (6): 634-638.

[17] Uyguroğlu R, Öztoprak AY. An alternative approach to the design of multiple beam constrained lens antennas. *Turkish Journal of Electrical Engineering & Computer Sciences* 2017; 25: 3334-3341. doi: 10.3906/elk-1606-215

[18] Rao JBL. Multifocal three dimensional bootlace lenses. *IEEE Transactions on Antennas and Propagation* 1982; 30 (6): 1050-1056. doi: 10.1109/TAP.1982.1142940

[19] Rappaport CM, Zaghloul AI. Optimised three-dimensional lenses for wide-angle scanning. *IEEE Transactions on Antennas and Propagation* 1985; 33 (11): 1227-1236. doi: 10.1109/TAP.1985.1143519

[20] Hansen RC, Bargeliotes PT, Boersma J, Chang ZW, Golden KE et al. Conformal Antenna Array Design Handbook. *NASA STI/Recon Technical Report*, 1981; 82: 21483.

[21] Wincza K, Gruszczynski S, Sachse K. Conformal four-beam antenna arrays with reduced sidelobes. *Electronic Letters* 2008; 44 (3): 174-175. doi: 10.1049/el: 20083423

[22] Mahmoodi A, Pirhadi A. Enhancement of scan angle using a Rotman lens feeding network for a conformal array antenna configuration. *Applied Computational Electromagnetics Society Journal* 2015; 30 (9): 959-966.

[23] Boyns JE, Munger AD, Provencher J, Reindel J, Small BI. A lens feed for a ring array. *IEEE Transactions on Antennas Propagation* 1967; 16 (2): 264-267. doi: 10.1109/TAP.1968.1139152

[24] Bodnar DG, Raider BK, Rahmat-Samii Y. Lens antenna concepts for land mobile satellite communications. *36th IEEE Vehicular Technology Conference; Dallas, TX, USA*, 1986; pp. 8-14. doi: 10.1109/VTC.1986.1623404

[25] Balanis CA. Antenna Theory Analysis and Design. 3rd ed. *Hoboken, NJ, USA: Wiley Interscience*, 2005.